Electronic Supplementary Material (ESI) for RSC Advances.
This journal is © The Royal Society of Chemistry 2023

Electronic Supplementary Information

Corrosion protection properties of tetraphenylethylene-based inhibitors toward carbon steel in acidic medium

Yumeng Chen,‡ Yiming An,‡ Jing Ma, Zhihua Zhang, Fulin Qiao, Xue Lei, Fei Sun*, Chunlu Wang*, Song Gao, Yue Zhao, Jinhua Wang, Xiaoping Fu, Hui Wang, Zhengqi Yu

Sinopec Research Institute of Petroleum Processing Co., Ltd., Beijing 100083, P. R. China

*Corresponding authors

sunfei.ripp@sinopec.com (Fei Sun)

wcl.ripp@sinopec.com (Chunlu Wang)

Contents

1. General Information

Tetraphenylethylene was purchased from Alfa Aesar. Raney Ni, $N_2H_4 \cdot H_2O$, NaSCN were purchased from Sinopharm Chemical Reagent Co., Ltd. HNO_3, H_2SO_4 and other reagents were analytical grade and purchased from Beijing Chemical Works. All the reagents were used without further purification.

^1H NMR and ^{13}C NMR spectra were recorded on Bruker Avance 400 MHz. High-resolution mass spectra (HRMS, ESI) were obtained with Bruker Solarix-FT-ICR MS. UV-Vis absorption spectra were recorded on a Perkin Elmer Lambda 750 Spectrophotometer. Fluorescence (FL) spectra were collected on a Hitachi F-7100 Fluorescence Spectrophotometer. X-ray photoelectron spectroscopy (XPS) spectra were studied on a Thermo Fisher Scientific Escalab Xi+ Spectrometer. Scanning electron microscope (SEM) images of brass coupons were studied on a Hitachi S-4800 Microscope.

Weight loss experiment procedures. Prior to the experiment, all carbon steel coupons were rinsed with absorbent cotton in ethanol and dried in cold air, then weighed by an electronic balance with precision of ± 0.1 mg. Then the coupons were immersed into 0.5 M H_2SO_4 solutions in the absence or presence of different concentrations of various compounds at 60 ^oC, steadily stirred by a magnetic stir bar. For each measurement, a freshly prepared solution was used. The immersion time for carbon steel coupons is 4 h. Then, the coupons were taken out from the corrosive medium and rinsed with absorbent cotton in chemical descaling solution (10% HCl + 0.5% Urotropin) and deionized water, dried in cold air and weighed with precision of ± 0.1 mg, successively. Afterwards, these coupons were used for XPS and SEM studies, respectively.

2. Synthesis and characterization

Upon variation of reactant ratios and reaction time, tetraphenylethylene (TPE) could be nitrated into different nitro-substituted tetraphenylethylenes (TPE-NO_2, TPE-$2NO_2$, TPE-$3NO_2$, and TPE-$4NO_2$) with HNO_3 and HOAc. Next, they were reduced to corresponding amino-substituted tetraphenylethylenes (TPE-NH_2, TPE-$2NH_2$, TPE-$3NH_2$, and TPE-$4NH_2$) in the presence of Raney Ni and $N_2H_4 \cdot H_2O$. Afterwards, they were respectively reacted with H_2SO_4, giving rise to the intermediate compounds. Subsequently, anion exchange reactions of these intermediates with NaSCN led to target compounds (**1**, **2**, **3** and **4**). Thereinto, nitro-substituted tetraphenylethylenes (TPE-NO_2, TPE-$2NO_2$, TPE-$3NO_2$, and TPE-$4NO_2$) and amino-substituted tetraphenylethylenes (TPE-NH_2, TPE-$2NH_2$, TPE-$3NH_2$, and TPE-$4NH_2$) were produced in line with literatures [S1-S5].

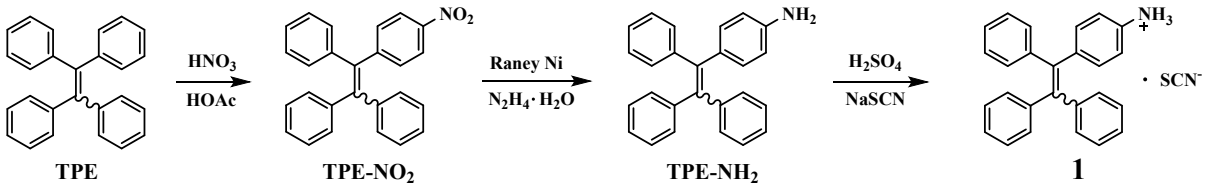

Synthesis of 1: In a 50 mL round-bottom flask, *p*-amino-tetraphenylethylene TPE-NH_2 (695 mg, 2.0 mmol) was dissolved in mixed solvent of acetone (10 mL) and ethanol (10 mL). Then, concentrated sulfuric acid (110 mg, 1.1 mmol) was added slowly, with emergence of insoluble sediment immediately. The mixture was stirred for 30 min and filtered. The residue was washed with ethanol for more than three times. Then, it was dispersed into ethanol (20 mL) in a 50 mL round-bottom flask. An ethanol (5 mL) solution dissolved with sodium thiocyanate (152 mg, 2.0 mmol) was added. The mixture was heated to 50 ^oC and stirred for 1

h. After being cooled to room temperature, the mixture was centrifuged and filtered. The organic phase was evaporated and dried in vacuum, to afford **1** as yellow solid (772 mg) in 94% yield. ^{1}H NMR (400 MHz, DMSO-d_6): δ 7.30 − 7.22 (1 H, m), 7.20 − 7.08 (9 H, m), 7.07 − 7.03 (2 H, m), 7.02 − 6.93 (6 H, m), 6.90 − 6.86 (1 H, d); ^{13}C NMR (100 MHz, DMSO-d_6): δ 143.24, 142.96, 142.80, 141.09, 140.29, 140.12, 139.46, 131.95, 130.93, 130.60, 129.56, 127.93, 126.67, 126.53, 121.75, 121.40; HRMS (ESI, positive): calcd. for $C_{26}H_{22}N$ (m/z): 348.17468; found: 348.17462.

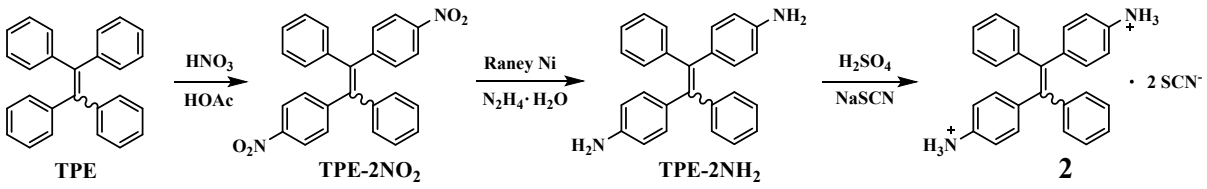

Synthesis of 2: In a 50 mL round-bottom flask, bis-*p*-amino-tetraphenylethylene TPE-2NH_2 (724 mg, 2.0 mmol) was dissolved in mixed solvent of acetone (15 mL) and ethanol (15 mL). Then, concentrated sulfuric acid (220 mg, 2.2 mmol) was added slowly, with emergence of insoluble sediment immediately. The mixture was stirred for 30 min and filtered. The residue was washed with ethanol for more than three times. Then, it was dispersed into ethanol (20 mL) was stirred in a 50 mL round-bottom flask. An ethanol (5 mL) solution dissolved with sodium thiocyanate (324 mg, 4.0 mmol) was added. The mixture was heated to 50 ^{o}C and stirred for 1 h. After being cooled to room temperature, the mixture was centrifuged and filtered. The organic phase was evaporated and dried in vacuum, to afford **2** as yellow solid (902 mg) in 94% yield. ^{1}H NMR (400 MHz, DMSO-d_6): δ 7.20 − 7.11 (6 H, m), 7.10 − 7.03 (8 H, m), 7.01 − 6.95 (4 H, d); ^{13}C NMR (100 MHz, DMSO-d_6): δ 142.76, 141.76, 138.45,

131.99, 131.55, 130.58, 129.78, 128.07, 126.88, 122.00; HRMS (ESI, positive): calcd. for $C_{26}H_{23}N_2$ [M − H^+] (m/z): 363.18558; found: 363.18574. calcd. for $C_{26}H_{22}N_2Na$ [M − $2H^+$ + Na^+] (m/z): 385.16752; found: 385.16772.

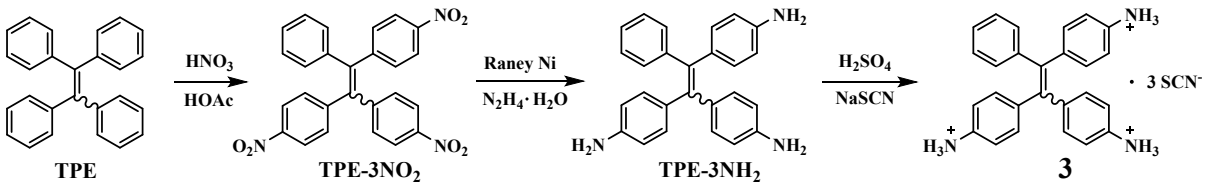

Synthesis of 3: In a 50 mL round-bottom flask, tri-*p*-amino-tetraphenylethylene TPE-$3NH_2$ (755 mg, 2.0 mmol) was dissolved in mixed solvent of acetone (15 mL) and ethanol (15 mL). Then, concentrated sulfuric acid (330 mg, 3.3 mmol) was added slowly, with emergence of insoluble sediment immediately. The mixture was stirred for 30 min and filtered. The residue was washed with ethanol for more than three times. Then, it was dispersed into ethanol (20 mL) was stirred in a 50 mL round-bottom flask. An ethanol (5 mL) solution dissolved with sodium thiocyanate (486 mg, 6.0 mmol) was added. The mixture was heated to 50 ^oC and stirred for 1 h. After being cooled to room temperature, the mixture was centrifuged and filtered. The organic phase was evaporated and dried in vacuum, to afford **3** as yellow solid (1045 mg) in 94% yield. ^1H NMR (400 MHz, DMSO-d_6): δ 7.34 − 7.21 (4 H, m), 7.20 − 7.06 (4 H, m), 7.05 − 6.95 (3 H, m), 6.94 − 6.76 (6 H, m); ^{13}C NMR (100 MHz, DMSO-d_6): δ 142.82, 140.90, 140.67, 140.11, 138.98, 133.68, 133.16, 132.73, 131.91, 130.60, 128.18, 128.03, 126.80, 121.26; HRMS (ESI, positive): calcd. for $C_{26}H_{24}N_3$ [M − $2H^+$] (m/z): 378.19647; found: 378.19655.

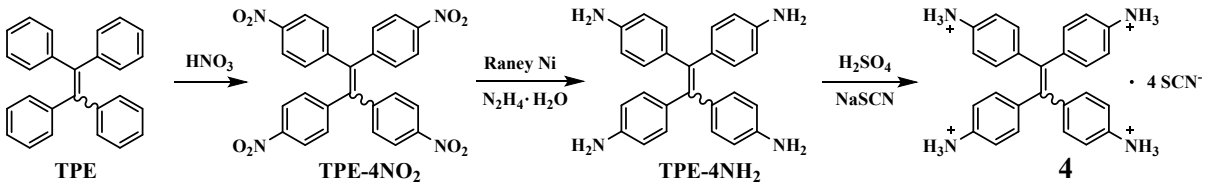

Synthesis of 4: In a 50 mL round-bottom flask, tetra-*p*-amino-tetraphenylethylene TPE-4NH_2 (785 mg, 2.0 mmol) was dissolved in mixed solvent of acetone (15 mL) and ethanol (15 mL). Then, concentrated sulfuric acid (440 mg, 4.4 mmol) was added slowly, with emergence of insoluble sediment immediately. The mixture was stirred for 30 min and filtered. The residue was washed with ethanol for more than three times. Then, it was dispersed into ethanol (20 mL) was stirred in a 50 mL round-bottom flask. An ethanol (5 mL) solution dissolved with sodium thiocyanate (649 mg, 8.0 mmol) was added. The mixture was heated to 50 ^{o}C and stirred for 1 h. After being cooled to room temperature, the mixture was centrifuged and filtered. The organic phase was evaporated and dried in vacuum, to afford **4** as yellow solid (1170 mg) in 93% yield. ^{1}H NMR (400 MHz, DMSO-d_6): δ 7.40 − 7.35 (8 H, d), 7.12 − 7.07 (8 H, d); ^{13}C NMR (100 MHz, DMSO-d_6): δ 140.94, 139.28, 131.98, 129.89, 121.56; HRMS (ESI, positive): calcd. for $C_{26}H_{25}N_4$ [M − 3H$^+$] (m/z): 393.20737; found: 393.20744.

3. Corrosion inhibitors for carbon steel in literature

Table S1. List of corrosion inhibitors for carbon steel in 0.5 M H_2SO_4 in literature.

Inhibitor	Concentration	Carbon steel	Method	Temperature	Inhibition efficiency	Mechanism of action	ΔG_{ads} (kJ/mol)	Adsorption isotherm	Reference
Methionine	10 mM	Carbon steel	EIS	25°C	85.92%				[S6]
2-amino-5-(3-pyridyl)-1,3,4-thiadiazole(3-APTD)	6 mM	Mild steel	EIS	30°C	92%		-33.36	Langmuir	[S7]
2-amino-5-(4-pyridyl)-1,3,4-thiadiazole (4-APTD)	6 mM	Mild steel	EIS	30°C	95%		-33.34	Langmuir	[S7]
Hexadecylpyridinium bromide (HDPB)	1 mM	Mild steel	EIS	60°C	91%	Mixed-type	-39.50	Bockris-Swinkels	[S8]
Polyaspartic acid (PASP)	2 g/L	Mild steel	Weight-loss	303 K	87.9%				[S9]
2-[4-(2-chlorobenzyl)-3-methyl-6-thiooxopyridazin-1(6H)-yl]acetohydrazide	25 mM	Steel	Weight-loss	298 K	99%		-18.76	Temkin	[S10]
N,N-Diethylammonium O,O'-di(4-bromophenyl)dithiophosphate (Br-NOP)	100 mg/L	Q235 steel	EIS	300 K	98.07%		-39.61	Langmuir	[S11]
Omeprazole (OMP)	300 mg/L	X60 Steel	EIS	298 K	92.52%		-26.06	Langmuir	[S12]
Mikania micrantha extract (MME)	100 mg/L	Cold rolled steel	Weight-loss	303 K	72.0%		-27.25	Langmuir	[S13]
3-phenyl-4-methylthiazol-2(3H)-thione	20 mM	Carbon steel	Weight-loss	303 K	95.0%	Mixed-type	-39.38	Langmuir	[S14]
3-(2-methyl-phenyl)−4-methylthiazol-2(3H)-thione	20 mM	Carbon steel	Weight-loss	303 K	91.3%	Mixed-type	-38.03	Langmuir	[S14]
3-(2-methoxyphenyl)−4-methylthiazol-2 (3H)-thione	20 mM	Carbon steel	Weight-loss	303 K	83.2%	Mixed-type	-31.90	Langmuir	[S14]
Alloxazine (ALLOX)	10 μM	Mild steel	Weight-loss	303 K	96.0%		-10.32	Temkin	[S15]
octylphenol polyethylene oxide (OPPEO)	50 mM	Low-carbon steel	EIS	303 K	95.0%		−40	Flory-Huggins	[S16]

4. SEM images

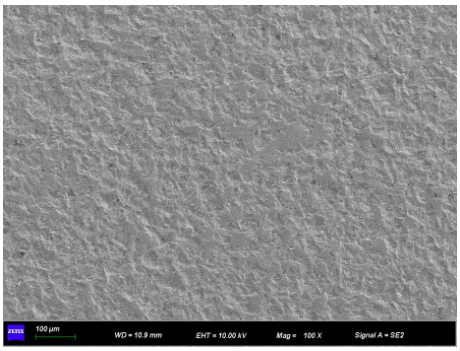

(a)

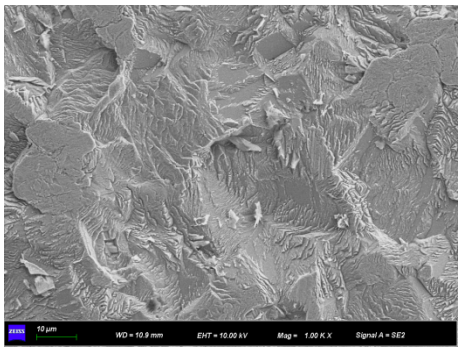

(b)

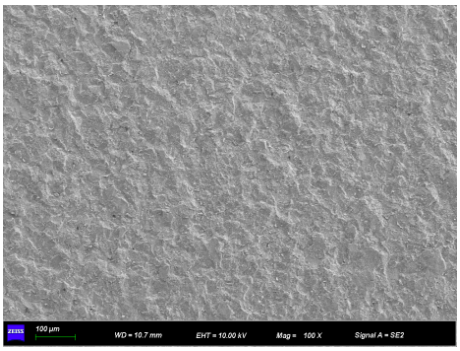

(c)

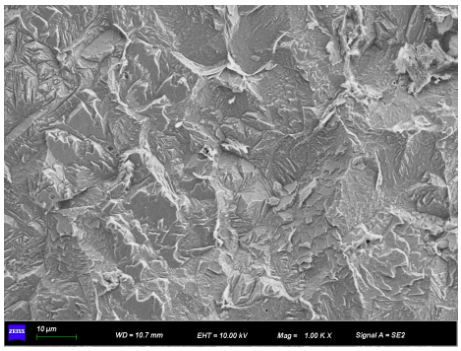

(d)

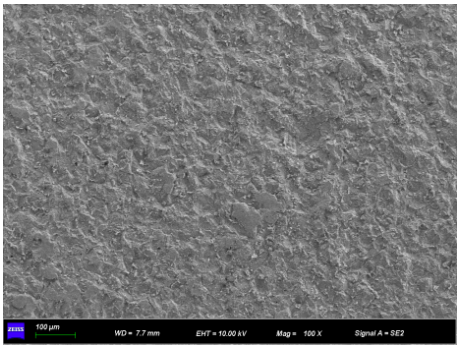

(e)

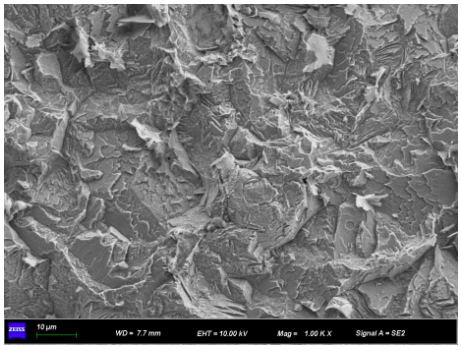

(f)

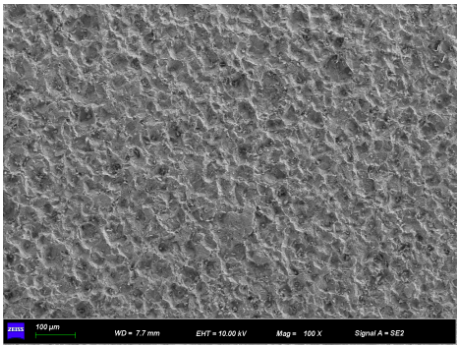

(g)

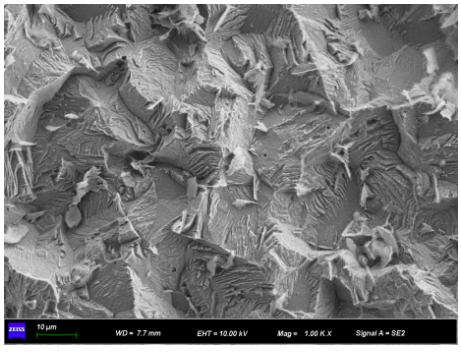

(h)

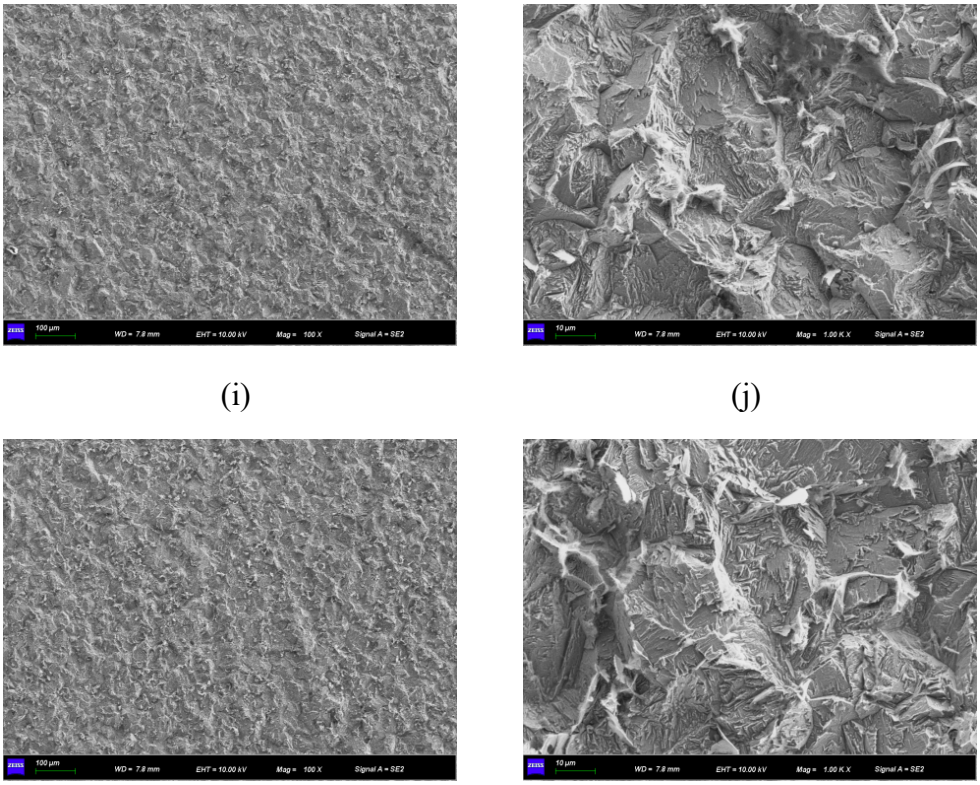

Fig. S1. SEM images of carbon steel coupons in the presence of increasing concentrations of **1** after weight loss measurements. (a, b) 5 mg/L; (c, d) 10 mg/L; (e, f) 20 mg/L; (g, h) 40 mg/L; (i, j) 70 mg/L; (k, l) 100 mg/L. Scale: 100 µm for (a, c, e, g, i, k) and 10 µm for (b, d, f, h, j, l).

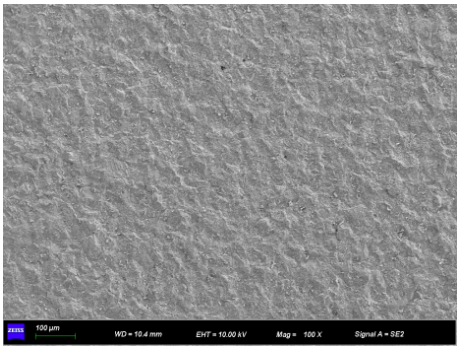

(a)

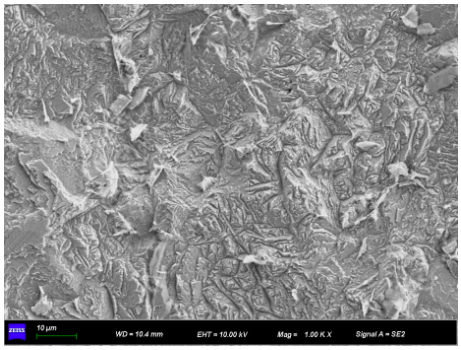

(b)

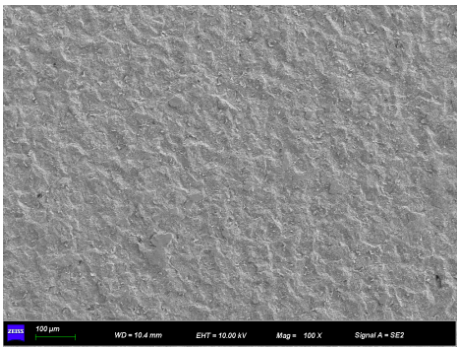

(c)

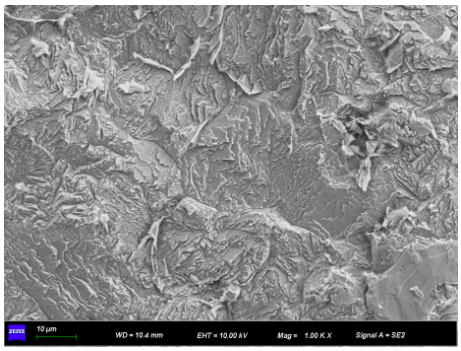

(d)

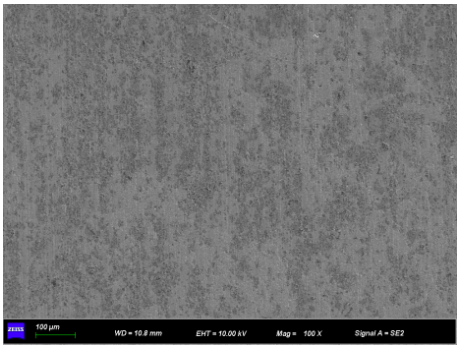

(e)

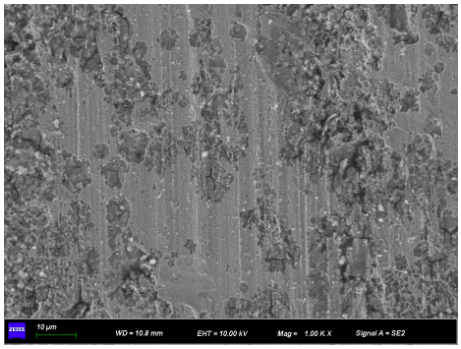

(f)

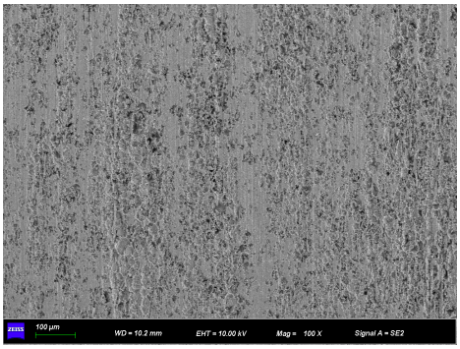

(g)

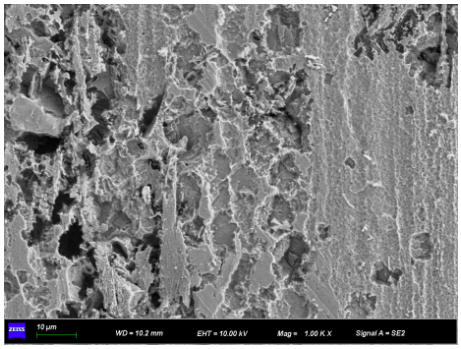

(h)

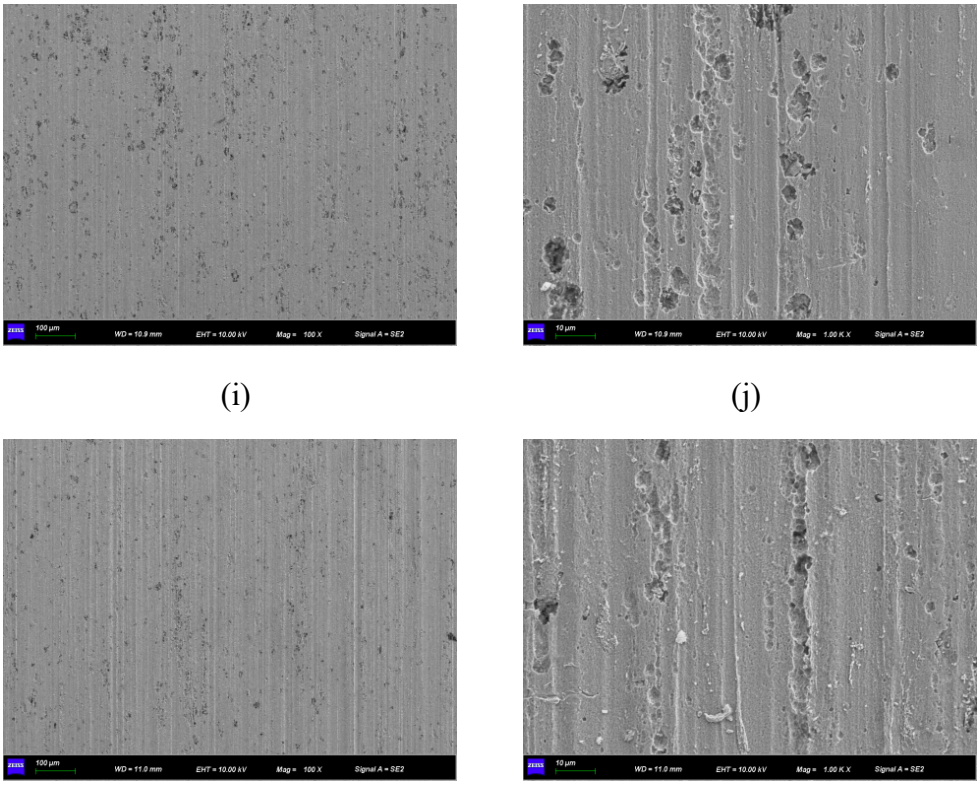

Fig. S2. SEM images of carbon steel coupons in the presence of increasing concentrations of **2** after weight loss measurements. (a, b) 5 mg/L; (c, d) 10 mg/L; (e, f) 20 mg/L; (g, h) 40 mg/L; (i, j) 70 mg/L; (k, l) 100 mg/L. Scale: 100 μm for (a, c, e, g, i, k) and 10 μm for (b, d, f, h, j, l).

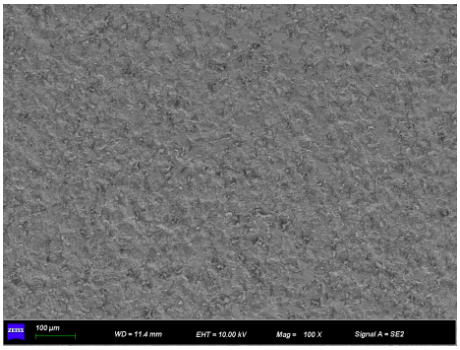

(a)

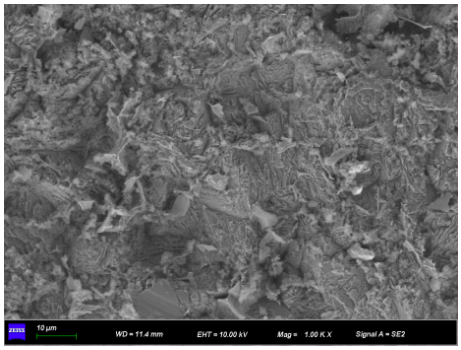

(b)

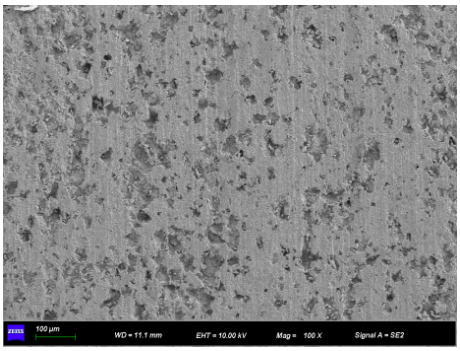

(c)

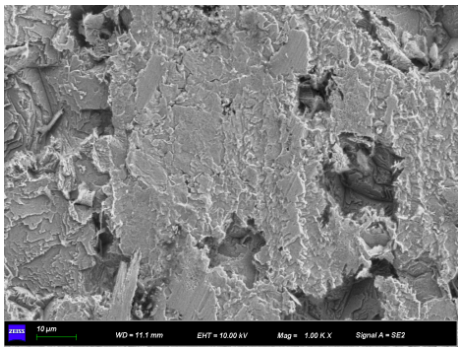

(d)

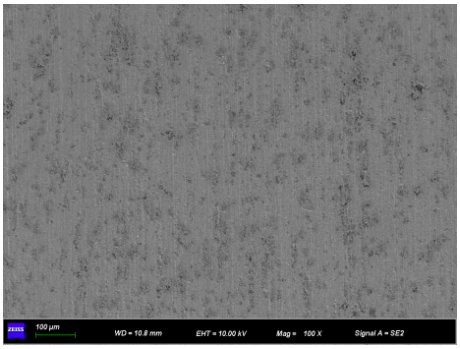

(e)

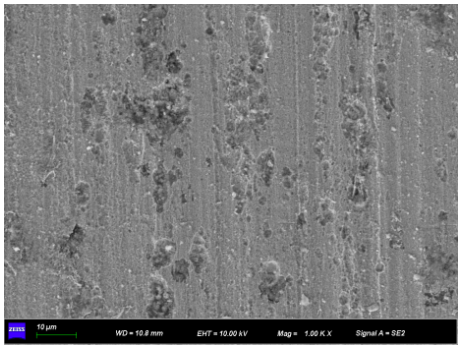

(f)

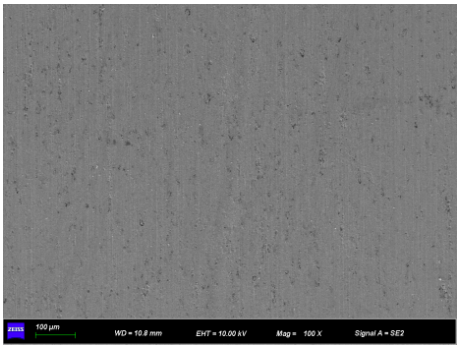

(g)

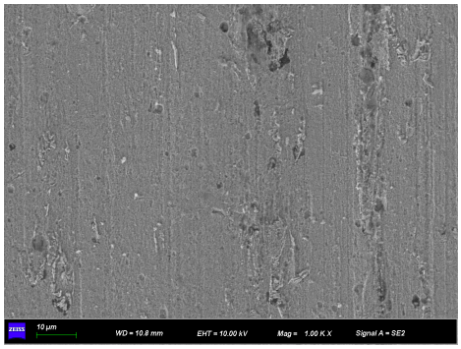

(h)

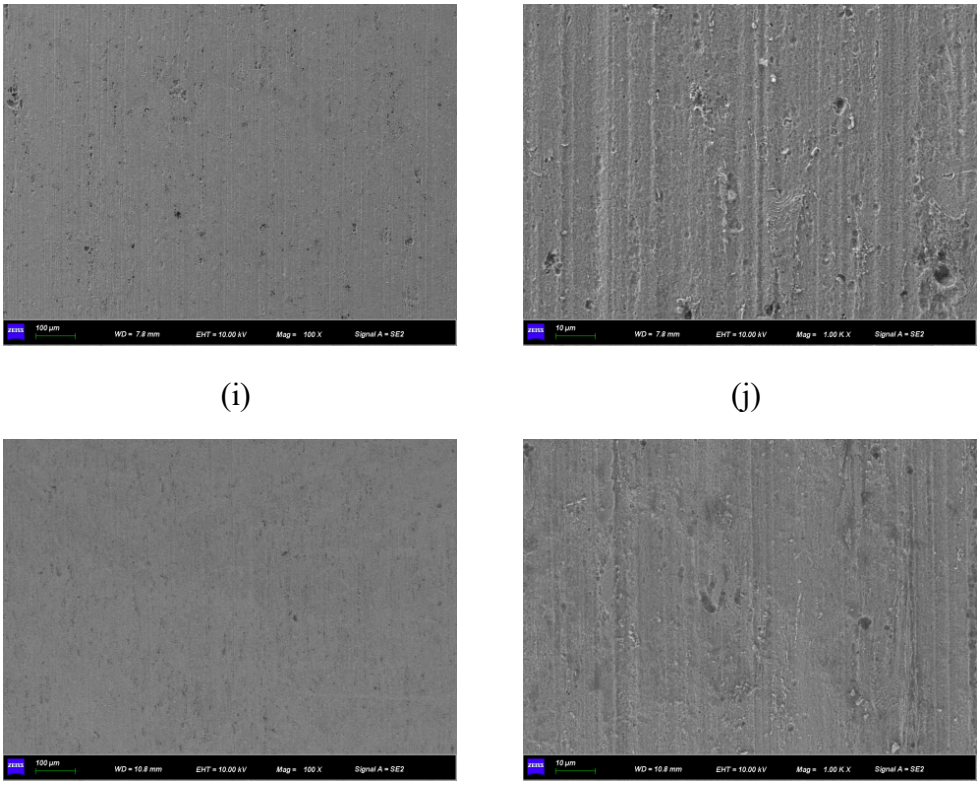

Fig. S3. SEM images of carbon steel coupons in the presence of increasing concentrations of **3** after weight loss measurements. (a, b) 5 mg/L; (c, d) 10 mg/L; (e, f) 20 mg/L; (g, h) 40 mg/L; (i, j) 70 mg/L; (k, l) 100 mg/L. Scale: 100 µm for (a, c, e, g, i, k) and 10 µm for (b, d, f, h, j, l).

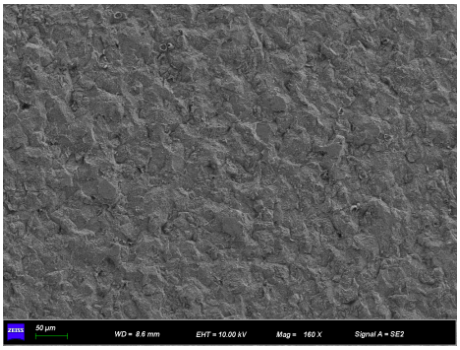

(a)

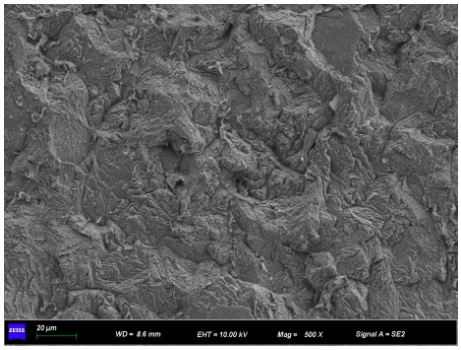

(b)

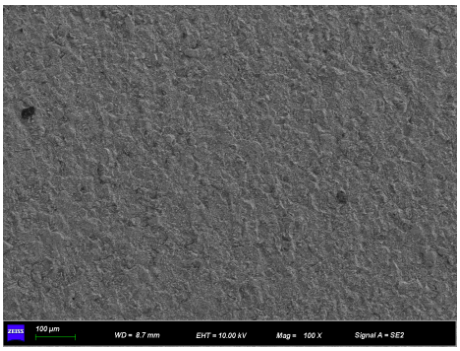

(c)

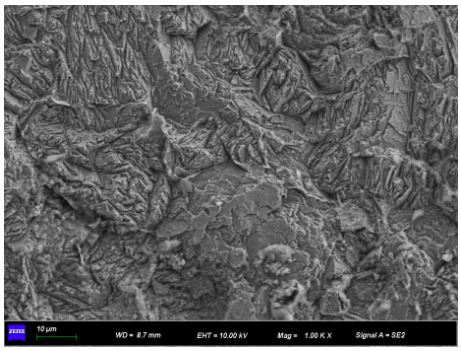

(d)

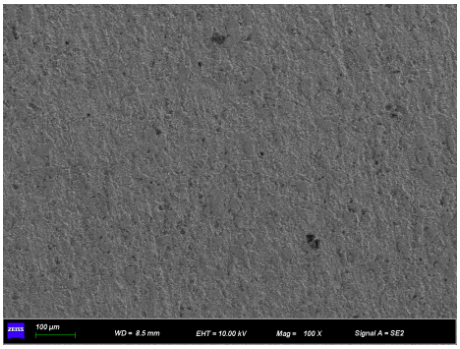

(e)

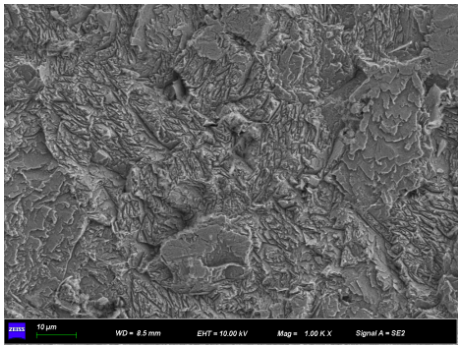

(f)

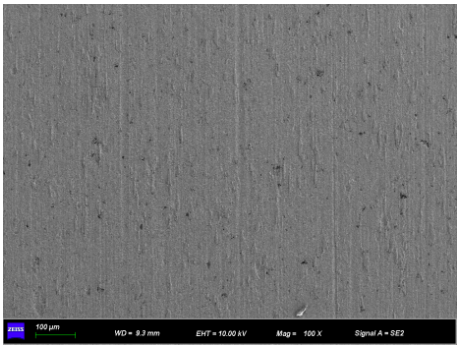

(g)

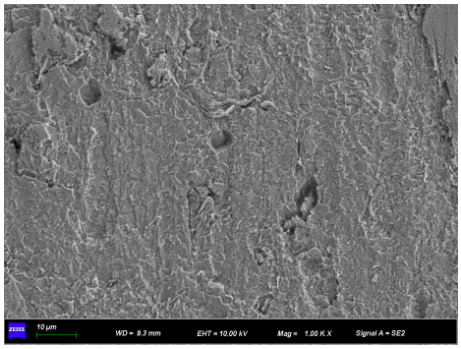

(h)

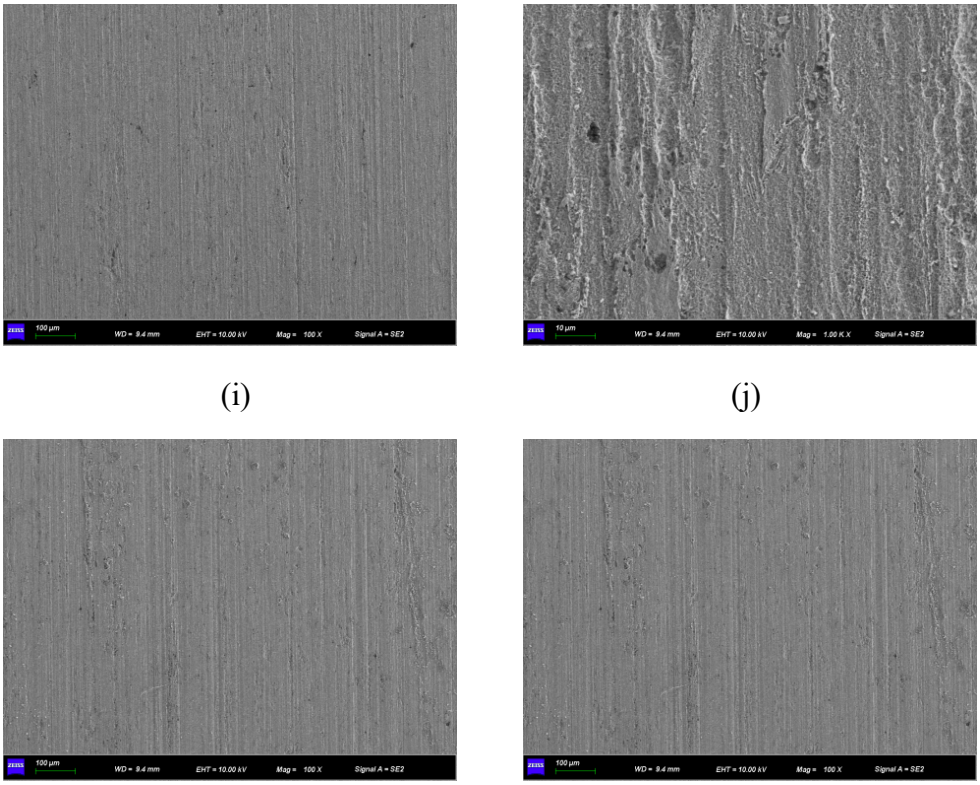

Fig. S4. SEM images of carbon steel coupons in the presence of increasing concentrations of **4** after weight loss measurements. (a, b) 5 mg/L; (c, d) 10 mg/L; (e, f) 20 mg/L; (g, h) 40 mg/L; (i, j) 70 mg/L; (k, l) 100 mg/L. Scale: 100 μm for (a, c, e, g, i, k) and 10 μm for (b, d, f, h, j, l).

5. Electrochemical measurements

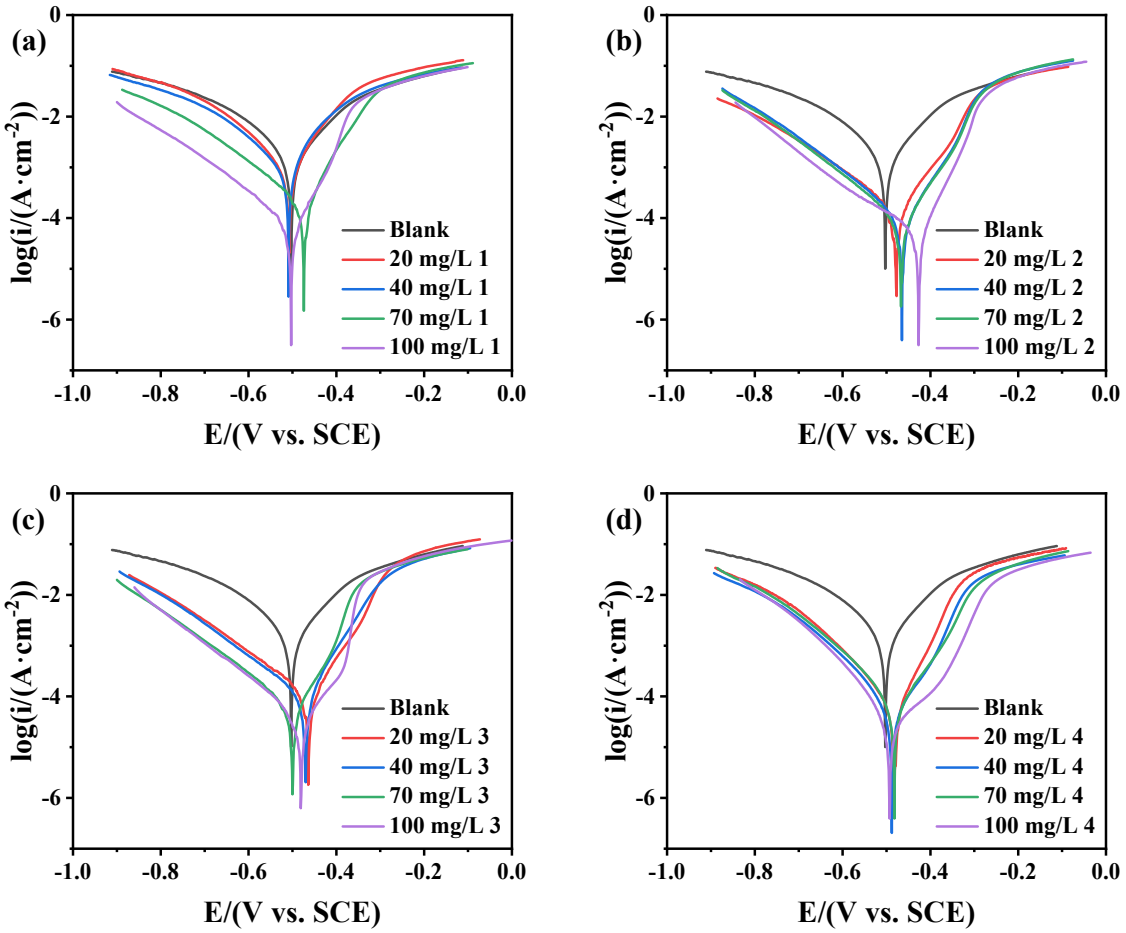

Fig. S5. PDP curves for carbon steel in the absence or presence of various concentrations of (a) **1**, (b) **2**, (c) **3** and (d) **4** in 0.5 M H_2SO_4.

Table S2. Electrochemical parameters of carbon steel in the absence or presence of different concentrations of TPE-based inhibitors by PDP measurements in 0.5 M H_2SO_4.

Inhibitor	c / (mg/L)	I_{corr} / (μA/cm^2)	E_{corr} / V	β_c / (mV/dec)	β_a / (mV/dec)	η_P / %
Blank	—	1701.0	-0.503	146.3	113.2	\
1	20	1006.0	-0.507	126.9	95.9	40.9
	40	1149.0	-0.509	132.9	102.0	32.5
	70	212.2	-0.474	145.1	75.7	87.5
	100	57.5	-0.502	141.7	48.1	96.6
2	20	166.2	-0.477	155.7	92.7	90.2
	40	97.3	-0.465	139.3	77.2	94.3
	70	97.3	-0.467	140.5	80.4	94.3
	100	55.1	-0.427	203.2	51.5	96.8
3	20	126.9	-0.464	165.4	81.8	92.5
	40	106.3	-0.470	160.1	74.8	93.8
	70	58.0	-0.500	145.8	50.7	96.6
	100	32.2	-0.481	140.7	44.5	98.1
4	20	43.7	-0.482	107.9	52.6	97.4
	40	44.7	-0.488	111.3	64.7	97.4
	70	65.1	-0.482	114.8	80.1	96.2
	100	35.6	-0.493	99.1	118.4	97.9

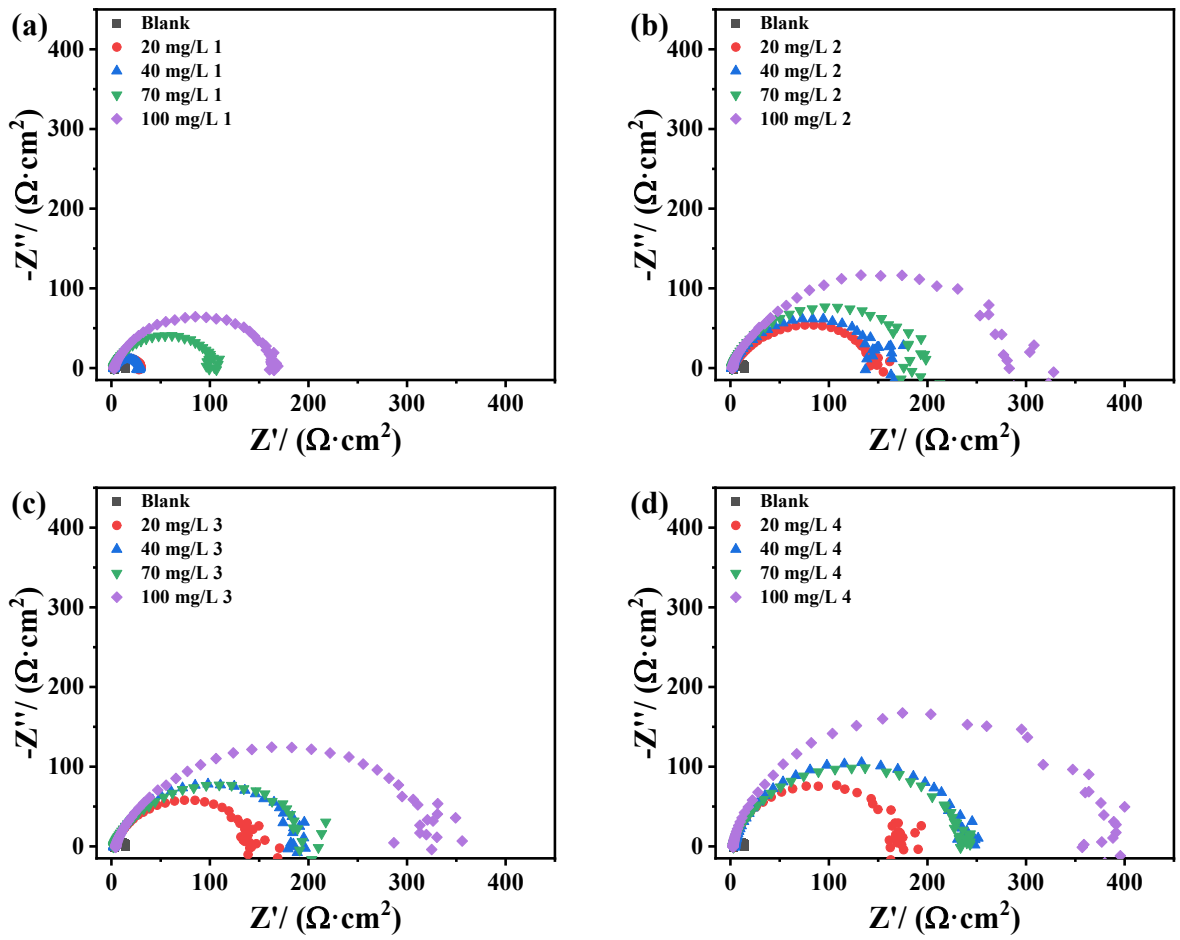

Fig. S6. EIS curves for carbon steel in the absence or presence of various concentrations of (a) **1**, (b) **2**, (c) **3** and (d) **4** in 0.5 M H_2SO_4.

Table S3. Electrochemical parameters of carbon steel in the absence or presence of different concentrations of TPE-based inhibitors by EIS measurements in 0.5 M H_2SO_4.

Inhibitor	c / (mg/L)	R_s / (Ω/cm^2)	R_{ct} / (Ω/cm^2)	η_E / %
Blank	—	2.7	11.8	—
1	20	2.0	27.66	57.3
	40	2.8	26.31	55.2
	70	2.1	105.6	88.8
	100	2.8	162.3	92.7
2	20	2.4	146.6	92.0
	40	1.6	156.5	92.5
	70	1.5	192.2	93.9
	100	1.9	287.9	95.9
3	20	3.0	140.1	91.6
	40	2.6	191.0	93.8
	70	2.2	201.2	94.1
	100	3.8	331.5	96.4
4	20	3.4	170.5	93.1
	40	3.9	237.9	95.0
	70	3.1	232.2	94.9
	100	3.0	383.0	96.9

Reference:

[S1] J.-B. Xiong, W.-Z. Xie, J.-P. Sun, J.-H. Wang, Z.-H. Zhu, H.-T. Feng, D. Guo, H. Zhang, Y.-S. Zheng, Enantioselective Recognition for Many Different Kinds of Chiral Guests by One Chiral Receptor Based on Tetraphenylethylene Cyclohexylbisurea, *J. Org. Chem.*, 2016, **81**, 3720-3726.

[S2] A. Schreivogel, J. Maurer, R. Winter, A. Baro, S. Laschat, Synthesis and Electrochemical Properties of Tetrasubstituted Tetraphenylethenes, *Eur. J. Org. Chem.*, 2006, **2006**, 3395-3404.

[S3] J. Lu, J. Zhang, Facile synthesis of azo-linked porous organic frameworks via reductive homocoupling for selective CO_2 capture, *J. Mater. Chem. A*, 2014, **2**, 13831-13834.

[S4] T. Yu, D. Ou, Z. Yang, Q. Huang, Z. Mao, J. Chen, Y. Zhang, S. Liu, J. Xu, M.R. Bryce, Z. Chi, The HOF structures of nitrotetraphenylethene derivatives provide new insights into the nature of AIE and a way to design mechanoluminescent materials, *Chem. Sci.*, 2017, **8**, 1163-1168.

[S5] W. Zhao, Z. He, Q. Peng, J. W. Y. Lam, H. Ma, Z. Qiu, Y. Chen, Z. Zhao, Z. Shuai, Y. Dong, B. Z. Tang, Highly sensitive switching of solid-state luminescence by controlling intersystem crossing, *Nat. Commun.*, 2018, **9**, 3044-3051.

[S6] G. L. F. Mendonça, S. N. Costa, V. N. Freire, P. N. S. Casciano, A. N. Correia and P. D. Lima-Neto, Understanding the corrosion inhibition of carbon steel and copper in sulphuric acid medium by amino acids using electrochemical techniques allied to molecular modelling methods, *Corros. Sci.*, 2017, **115**, 41-55.

[S7] Y. Tang, X. Yang, W. Yang, R. Wan, Y. Chen and X. Yin, A preliminary investigation of corrosion inhibition of mild steel in 0.5M H_2SO_4 by 2-amino-5-(n-pyridyl)-1,3,4-thiadiazole: Polarization, EIS and molecular dynamics simulations, *Corros. Sci.*, 2010, **52**, 1801-1808.

[S8] M. M. Saleh, Inhibition of mild steel corrosion by hexadecylpyridinium bromide in 0.5 M H_2SO_4, *Mater. Chem. Phys.*, 2006, **98**, 83-89.

[S9] B. Qian, J. Wang, M. Zheng and B. Hou, Synergistic effect of polyaspartic acid and iodide ion on corrosion inhibition of mild steel in H_2SO_4, *Corros. Sci.*, 2013, **75**, 184-192.

[S10] M. Bouklah, N. Benchat, A. Aouniti, B. Hammouti, M. Benkaddour, M. Lagrenée, H. Vezin and F. Bentiss, Effect of the substitution of an oxygen atom by sulphur in a pyridazinic molecule towards inhibition of corrosion of steel in 0.5M H_2SO_4 medium, *Prog. Org. Coat.*, 2004, **51**, 118-124.

[S11] C. Lai, X. L. Su, T. Jiang, L. Zhou, B. Xie, Y. Li, L. Zou. Corrosion inhibition of q235 steel in H_2SO_4 solution by n,n- diethylammonium o,o'-di(4-bromophenyl) dithiophosphate, *Int. J. Electrochem. Sci.*, 2016, **11**, 9413-9423.

[S12] Y. Liu, W. Du, X. Yao, C. Liu, X. Luo, L. Guo, C. Guo, Electrochemical and Theoretical Study of Corrosion Inhibition on X60 Steel in H_2SO_4 Solution by Omeprazole, *Int. J. Electrochem. Sci.*, 2022, **17**, 220516.

[S13] M. Tang, X. Li, S. Deng and R. Lei, Synergistic inhibition effect of Mikania micrantha extract with KI on steel corrosion in H_2SO_4 solution, *J. Mol. Liq.*, 2021, **344**, 117926.

[S14] O. Benali, M. Zebida, F. Benhiba, A. Zarrouk and U. Maschke, Carbon steel corrosion inhibition in H_2SO_4 0.5 M medium by thiazole-based molecules: Weight loss, electrochemical,

XPS and molecular modeling approaches, *Colloids Surf. A Physicochem. Eng. Asp.*, 2021, **630**, 127556.

[S15] N. O. Obi-Egbedi and I. B. Obot, Inhibitive properties, thermodynamic and quantum chemical studies of alloxazine on mild steel corrosion in H_2SO_4, *Corros. Sci.*, 2011, **53**, 263-275.

[S16] A. S. Algaber, E. M. El-Nemma and M. M. Saleh, Effect of octylphenol polyethylene oxide on the corrosion inhibition of steel in 0.5 M H_2SO_4, *Mater Chem. Phys.*, 2004, **86**, 26-32.